MASSACHUSETTS INSTITUTE OF TECHNOLOGY
HAYSTACK OBSERVATORY
WESTFORD, MASSACHUSETTS 01886
February 10, 2020

Telephone: 617-715-5517
Fax: 617-715-0590

To: IVS VGOS Correlation Groups

From: J. Barrett, R. Cappallo, B. Corey, P. Elosegui, D. Mondal, A. Niell, C. Ruszczyk, and M. Titus

Subject: Comparison of correlator results from VGOS intensive VI9290 test

1 Introduction

We used data from the one hour intensive session VI9290 (2019/10/17) between the VGOS antennas at KPGO (K2) and Wettzell (Ws) to compare correlation results from each of the participating correlation centers. The session was processed as a blind test by five VGOS correlators – MIT Haystack, Bonn, Vienna, WACO, and Shanghai – to assess correlator readiness for standard operational VGOS processing. All correlators used the DiFX and HOPS software packages to, respectively, correlate and post-process the data following the procedures described in [1]. Because the data, processing software, and methods were all the same, one would expect (close to) identical results all through the data path, from correlation to geodetic estimates. Preliminary results from the geodetic processing of the individual databases had uncovered larger-than-expected inter-correlator differences [2], so further investigation was desirable to locate where discrepancies may have been introduced. For the purpose of this study MIT Haystack was used as the reference correlator during comparison.

2 Methods

To determine where differences were introduced during the correlation and subsequent post-processing, several quantities were examined to compare the values obtained by each correlation center. This was done by considering the following topics/questions.

1. **Correlator setup:** What software versions were used? Were there any large differences in how the correlation was done?
2. **Clock model:** Compare the clock model used for correlation. What are the clock offset and rate for each station? What is the net clock rate and net rate relative to the reference correlator (MIT Haystack)?
3. **Control file:** What are the differences between the control files use for post-processing? Namely, what are the differences in the applied manual phase-cal (pc_phases) values and the Y-X polarization phase and delay offsets?
4. **Data Quality:** What does the basic data quality from each correlation center look like? What is the relative frequency of each quality code? How does the SNR of each scan compare among the correlation centers?
5. **Total multi-band delay:** How do the values of the total multi-band delay found for each scan compare among correlation centers? Are they consistent with each other? Are there any outliers or severe discrepancies?
6. **Residual multi-band delay:** If we compare the residual multi-band delay between each correlation center and the reference correlator, is the residual multi-band delay difference, as a function of time, consistent with the relative net rate between the two correlators' clock models?
7. **dTEC:** How well does the dTEC determined from each scan compare between each correlation center and the reference?
8. **Proxy cable-cal.:** Are the proxy cable-cal delay values derived from each scan consistent among the correlators?
9. **Control file cross comparison:** How sensitive are the total multi-band delay results to the control file used? For example, if the data correlated by the other correlation centers are fringe-fit using MIT Haystack's control file, do the data exhibit the same features (e.g. total multi-band delay differences and outliers)?

3 Results

The results of these comparisons are summarized below and grouped by original topic.

1. **Correlator setup:** There were some differences in the software versions of DiFX and HOPS used by each correlator. This is summarized in table 1. The site positions are summarized in table 2. Though there wasn't agreement among all four correlators, the site positions used for each station were identical for MIT and Vienna, and separately, identical for Bonn, Waco and Shanghai. The Earth orientation parameter (EOP) model used by each correlator also had some differences in both epoch and in the parameter values. Each correlator specified five days worth of EOP parameters. However, the parameter values of MIT and WACO spanned the days 289-293, while Bonn's and Shanghai's spanned 288-292, and Vienna's spanned 290-294. Figures 1, 2, and 3 show the values of UT1-UTC, and the X and Y polar positions used in the EOP model of each correlator.

2. **Clock model:** The differences between the correlator clock models is summarized in table 3. This table shows that with the exception of Shanghai, the net clock offset (K2 offset - Ws offset) found by each correlation center is similar to within approximately 1 nanosecond, while the net clock rate (K2 rate - Ws rate) ranges from -1.7 ps/s to 0.6 ps/s. The clock model epoch was the same for Bonn, Vienna, WACO and Shanghai but different from MIT's epoch, which was set 18.5 hours earlier.

3. **Control file:** Post-correlation, the fourfit control files contain several parameters to guide fringe-fitting which can have a large impact on the multi-band delay. Namely at issue are the values of the Y-X polarization phase and delay offsets, and the manual phase-cal (pc_phases) applied for each station. Table 4 summarizes the differences in the Y-X polarization phase/delay offsets found by each correlator. For the most part, the Y-X delay and phase offsets are quite similar. The Y-X delay offset found by each correlation center for K2 differs by no more than 4 ps, while for Ws it differs no more than 5 ps. Similarly, the Y-X phase offset of K2 found by each correlation center are all within 1.5 degrees of each other, while for Ws, they are all within 2.3 degrees. Larger differences are noticed in the values of the channel-by-channel manual phase-cal offset (pc_phases) applied to each station-polarization. Figures 5 to 8 show the pc_phases applied to each station and polarization. The most obvious difference to be noted here is that for any particular station-polarization, one or more correlators have derived non-zero pc_phases, while others have set them to zero. The reasons for this are somewhat complicated, but primarily boil down to: (1) the choice of network-reference station was not consistent among all correlation centers, (2) a priori values for the pc_phases have not been used everywhere, and (3) there is a minor bug in the control file generation script[1]. In the case of this test, MIT, Bonn, Vienna, and Shanghai chose Kokee as the network phase-reference station, while WACO chose Wettzell as the reference station. While this choice is arbitrary, in the case of this test, due to issues (2) and (3) it did affect the determination of the pc_phases, and subsequently, the fringe-fitting. Furthermore, MIT did not process this session like the other correlators, but in fact used a control file derived from a 24 hour VT-session in which GGAO (X-pol) was used as the network phase reference[2]. Vienna and Shanghai did not use any a priori phase corrections (either for Kokee or Wettzell), which usually makes the results of the first pass fringe fitting generally quite poor[3]. When no a priori pc_phases are set in the initial control file, this leads to a reduction in SNR and sometimes dTEC disagreements between different polarization products. This reduces the amount of data which can be used to make fresh estimates of the station pc_phases for the session of interest. Given that there is only about an hour of data to work with for VI9290, it's not altogether too surprising that the control file generation script was unable to find enough scans which pass all the various cuts (SNR, q-code, and dTEC similarity between all 4 polarization-products) in order to derive Y-pol pc_phases for Kokee (Vienna/Shanghai's choice as reference station). Deriving the Y-pol pc_phases for the reference station requires either more or better quality data, since deriving the pc_phases from any particular scan requires a good fringe on at least two polarization products (XX-YX or XY-YY). Whereas determining the pc_phases for a non-reference station only needs to have a good fringe on one of two polarization products XY or XX (depending on the polarization of interest). On account of this, while Vienna and Shanghai did obtain estimates for Wettzell's pc_phases, their control file has no pc_phases applied to Kokee. Further complicating the comparison of the correlator control files is the fact that WACO and Bonn both used a priori pc_phases, but chose different reference stations. This fact, combined with the aforementioned bug in the control file generation script, caused Bonn to produce a control file with the Kokee X-polarization pc_phases set to zero, while WACO ended up with Wettzell X-polarization pc_phases set to

[1] Due to this bug, when a station is chosen as the network phase reference station and if a priori pc_phases are applied to this station by the user, these a priori pc_phases are not carried over for the X-polarization and are instead reset to zero in the produced control file. The appropriate behavior should be to insert these a priori pc_phases into the resulting control file unmodified. This is of no effect during the normal processing of VT sessions, as the nominal network reference station is not supposed to have any pc_phases applied to the X-polarization channels.

[2] This is the reason why MIT's pc_phases are non-zero for every station-polarization as shown in figures 5 to 8.

[3] However, it is important to point out the need for a priori pc_phases was not stressed in the VGOS data processing manual[1].

zero. Correcting these differences in the control files will require a minor software fix, but also consistent use of a priori pc_phases, and a uniform way of selecting the network phase reference station.

4. **Data Quality:** The overall comparison of the quality of the data produced by each correlation center is summarized in table 5. A comparison of the SNR of each scan by correlation center is shown in figure 4. This shows that there are some discrepancies in SNR. Mostly the differences are small (the median percent differences in SNR, with respect to the reference, for each correlator are 0.86%, 3.61%, 2.68%, and 0.94% for Bonn, Vienna, WACO, and Shanghai respectively). However, there are a few outliers where the SNR differs drastically from the reference correlator by more than 100%. These outliers are discussed further in the following section. Note that WACO did not correlate scans after 290-1919 due to trouble in de-muxing the raw data. Similarly, Shanghai did no correlate scans after 290-1926.

5. **Total multi-band delay:** To compare the total multi-band delay found by each correlation center with the reference correlator, the total multi-band delay difference ($\Delta\tau_{MBD}$) for each scan has been histogrammed in figures 9,10, 11, and 12. In addition, the total multi-band delay difference is plotted as a function of time, since the start of the session for each correlation center compared with the reference in figures 13,14, 15, and 16. These show that the general trend in the total multi-band delays found by each correlator exhibits an offset (a few to tens of picoseconds) and negligibly small rate (< 0.001 ps/s). In these plots, we have chosen to show the mean offset and standard deviation but have ignored any small non-zero rate. However, one feature that is somewhat concerning, is the presence of a handful of scans which have extremely large differences between the total multi-band delay found by each correlator. The difference in total multi-band delay for these outliers can range from 100s to 10s of thousands of picoseconds. The scans selected as outliers are listed in the annotations underneath each figure, along with the mean and standard deviation. In order to identify these outliers, the modified z-score method based on the median absolute deviation (MAD) was used (see [3]). Scans with a modified z-score greater than 20 were flagged as outliers. Table 6 summarizes these outlier scans for each correlator. Investigation of the raw station data files from these outlier scans has determined that some of the data from Wettzell may have been corrupted during the process of running `vmux` to convert the multi-threaded VDIF data to single-threaded VDIF. Specifically, scans 290-1853 and 290-1927 (at least when converted at MIT) suffered from a large amount of fill pattern in the Wettzell data (in excess of what is already present in the original data), which likely corrupted the results of these scans. It is possible this problem may have affected these scans (as well as others) in a different way at each of the other correlation centers. In order to know if that is the case, the raw data will need to be inspected in closer detail. In addition, there are some scans (290-1901, 290-1906, 290-1912) where the discrepancy in the multi-band delay seems to be associated with the mis-fitting of the dTEC. The underlying cause of these dTEC differences may also be the data de-muxing problem occurring at one or more of the correlators, or perhaps, more likely, it is due to differences in the applied pc_phases. However, this needs further investigation to determine the cause with certainty.

6. **Residual multi-band delay:** A comparison of the residual multi-band delays (the correction to the correlator delay model found by fourfit) found by each correlation center with respect to the reference correlator is shown in figures 17, 18, 19, and 20. These plots show that the trend of the residual multi-band delay difference exhibits a rate consistent with the relative net clock rate of the two correlator's clock models. Since the scatter in the residual multi-band delay differences is generally much greater, there are fewer scans which are flagged as outliers as opposed to the total multi-band delay differences. In this case there is only one very problematic scan – 290-1927, which is known to have suffered data corruption.

7. **dTEC:** The differences in the dTEC found for each scan between the correlators is generally small. The differences are histogrammed in figures 21 to 24. However, there are a few outliers where the dTEC fitting procedure has failed to find a consistent value. Most of these are the same outlier scans identified before which may have diverged due to data corruption and/or to the differences in the pc_phases applied by each correlator.

8. **Proxy cable-cal.:** Figures 25 and 26 show the proxy cable-cal. delay derived for Kokee and Wettzell respectively by each correlation center. For the most part, the differences are negligible since three of the correlation centers (MIT, Bonn, Vienna) chose the same band-polarization combinations (BCD, both pols.) to use when computing the proxy cable-cal. delay. However, WACO and Shanghai chose a slightly different set of band-polarizations[4], which leads to differences on the order of a few picoseconds.

9. **Control file cross comparison:** The correlated data (in Mk4 format) from each correlation center was re-fringed using the reference correlator's control file in order to get an idea of how much the control file settings (pc_phases, Y-X phase/delay offsets) may have affected the total multi-band delay results. The time trend of the total multi-band delay differences for each correlator are shown in figures 27, 28, 29, and 30. In

[4]WACO chose all four bands (ABCD) and both polarizations, while Shanghai chose both polarizations and all four bands (ABCD) for Kokee, but only bands BC for Wettzell.

these figures, it is seen that some of the same problematic outlier scans are still present (290-1853, 290-1927) as before, which is likely due to corruption of the raw data. However, it should also be noted that there were two additional scans selected as outliers for WACO (290-1849, and 290-1912). Table 7 summarizes the mean, standard deviation, and WRMS scatter of $\Delta\tau_{MBD}$ for each correlation center's data when processed with either their own native control file or with MIT's control file. In this case the WRMS scatter is defined as

$$WRMS = \sqrt{\left(\frac{N_{obs}}{N_{dof}}\right)\left(\frac{1}{W_{tot}}\right)\sum_i \frac{(\tau_i(a) - \tau_i(r))^2}{\sigma_i^2(a)}} \tag{1}$$

for correlator's a and r, where $\tau_i(a)$ is the total multi-band delay of scan i for correlator a and r denotes reference correlator. The formal MBD error reported by fourfit is denoted by $\sigma_i(a)$, while $W_{tot} = \sum_i \frac{1}{\sigma_i^2(a)}$. Here N_{obs} is the number of scans while $N_{dof} = N_{obs} - 1$.

4 Conclusion

The data processing of several correlation centers was compared for a VGOS intensive session between the VGOS antennas at Wettzell and Kokee without coordination. In this process, it was discovered that there are several places during data processing where solutions may diverge. The first of these is the correlator clock model for each station. In the case of this test, it appears that while the station peculiar offsets differed among the several correlators, the net offset was quite close ($\sim$ 1ns). With some coordination between the correlators, the individual station peculiar offsets could be brought closer into alignment. The net clock rate found by each correlator varied from, -1.7 ps/s to 0.6 ps/s. It is possible the difference between the correlators may be attributed to the fact that for a short 1-hour intensive session there is simply less data to make a precise clock rate determination, as evidenced by the fact that even for the correlators which chose the same clock model epoch, the differences in the net rate were up to $\sim$ 2.3ps/s.

Excluding outliers, by and large, the differences in SNR and total multi-band delay as found by each correlator are relatively small and likely have their origins in the differences between the control files used for fringe fitting. While the station Y-X phase/delay offsets derived by each correlator were largely in agreement with each other, the manual phase cal. offsets (pc_phases) had more variation. Generally speaking, the pc_phases for each station were similar to within $10 - 15$ degrees. However, this could have been greatly improved through the use of a priori pc_phases in the initial control file. In addition, one correlator chose the opposite convention from the others for the network phase reference station. Since this choice is arbitrary, it may help to have the choice of network reference station assigned via some yet-to-be-determined convention or coordinated among the centers, in order to maintain better agreement in the pc_phases values among correlators.

Upon examining the total multi-band delay differences ($\Delta\tau_{MBD}$) of each scan among the correlators, it was found that there were a handful of scans which exhibited very large differences ($> 10^4$ps). These differences may possibly be explained by corruption of the raw station data during the conversion of the raw multi-threaded VDIF data to the single-threaded VDIF format. However, more investigation of the raw data is needed to determine if this is case and/or if this problem affected other scans. In addition, a few scans exhibited more moderate $\Delta\tau_{MBD}$ of 100s of ps, which appears to be due to different dTEC solutions being found by the correlators. This may occur for low SNR scans if the pc_phases applied by each correlator differ enough. However, excluding the aforementioned outlier scans, by and large the differences of the total multi-band delay found for each scan between the correlators which chose the same network reference station, were generally in the range of a few to tens of picoseconds. The mean $\Delta\tau_{MBD}$ among the correlators which chose the same reference station (Bonn, Vienna, Shanghai) was somewhat clustered between -10 to -15 ps, whereas the mean $\Delta\tau_{MBD}$ for WACO (which chose a different network reference station) was larger by nearly 20 ps. When the data of each correlation center was re-fringed with the same control file it was noted that, with two exceptions[5], both the mean, standard deviation, and WRMS of $\Delta\tau_{MBD}$ were largely reduced, as shown in table 7, though the most notable difference is the reduction of the mean difference to roughly 1 ps or less.

In addition, further differences were introduced during the application of the proxy cable-calibration. The differences in the proxy cable-cal. delays were generally quite small ($<$ 1ps) as long as the correlators choose the same bands-polarizations to average together. However when this is not the case, differences of several picoseconds can be introduced by this step. Future use of this tool should be made more consistent either by automating the selection of band-polarizations or by establishing firm rules to aid this selection. On the other hand, the need for this tool could be obviated if all antennas were equipped with a cable delay measurement system.

In conclusion, in addition to checking that the raw data being processed by each correlator does not suffer from corruption, there are a few changes to the data processing procedure which could be attempted to obtain better consistency between the correlation centers. These would be:

[5] While the offset was reduced, the standard deviation of ($\Delta\tau_{MBD}$) for Bonn and Vienna increased by 0.8 and 1.1 ps respectively when re-fringed with MIT's control file.

1. Make sure the station peculiar offsets are coordinated between the correlators and establish a uniform procedure for setting station clock epochs and rates.

2. If the station data is e-transfered and de-threaded using `vmux` (or otherwise), it should be checked for data loss or corruption before correlation[6].

3. The importance of a priori pc_phases in the initial first-pass control file should be stressed. Some mechanism (correlator reports?) should be used to communicate the a priori pc_phases information.

4. The control file generation scripting should be fixed to ensure that a priori phases for the X-pol. of the network station are carried over to the production control file.

5. Specify rules for the selection of an alternate network phase reference station when the primary station is not available.

6. Specify how to select, or automate, the band-polarization choices for the proxy cable-cal. delay.

Once the above recommendations are implemented, they will be incorporated into the VGOS data processing manual [1] and post-processing software.

References

[1] J. Barrett, R. Cappallo, B. Corey, G.B. Crew, P. Elosegui, A. Niell, C. Ruszczyk, and M. Titus. VGOS Data Processing Manual version 1.1, 2019. URL: `ftp://ivs.bkg.bund.de/pub/vgos_corr_workshop/vgos-data-processing.pdf`.

[2] S. Bolotin. Personal communication, 2019.

[3] I Boris and D Hoaglin. How to Detect and Handle Outliers, the ASQC Basic References in Quality Control: Statistical Techniques, 1993.

[6]This could be done using `dqa` or equivalent.

Correlator	DiFX version	HOPS version
MIT	2.5.2	3.21
Bonn	2.6.1	3.20
Vienna	2.5.2	3.20
WACO	2.6.1	3.20
Shanghai	2.5.2	3.20

Table 1: Correlator software version summary.

Correlator	K2 position (X,Y,Z) (m)	Ws position (X,Y,Z) (m)
MIT	$(-5543831.405,\ -2054585.733,\ 2387828.797)$	$(4075659.227,\ 931824.891,\ 4801516.193)$
Bonn	$(-5543831.705,\ -2054585.983,\ 2387828.776)$	$(4075659.100,\ 931824.640,\ 4801516.180)$
Vienna	$(-5543831.405,\ -2054585.733,\ 2387828.797)$	$(4075659.227,\ 931824.891,\ 4801516.193)$
WACO	$(-5543831.705,\ -2054585.983,\ 2387828.776)$	$(4075659.100,\ 931824.640,\ 4801516.180)$
Shanghai	$(-5543831.705,\ -2054585.983,\ 2387828.776)$	$(4075659.100,\ 931824.640,\ 4801516.180)$

Table 2: Site positions used by each correlator.

Quantity	MIT	Bonn	Vienna	WACO	Shanghai
Epoch	2019y290d00h00m	2019y290d18h30m	2019y290d18h30m	2019y290d18h30m	2019y290d18h30m
K2 offset (μs)	9.163	8.668	8.662	9.106	8.660
Ws offset (μs)	0.524	0.028	0.020	0.467	-0.0446
Net offset (K2-Ws) (μs)	8.639	8.640	8.640	8.639	8.705
Relative net offset w.r.t MIT (μs)	–	0.001	0.001	0.001	0.066
K2 rate (ps/s)	-0.422	-1.360	-1.704	-1.422	0.6
Ws rate (ps/s)	-0.002	-0.135	0.0	-0.06642	0.0
Net rate (K2-Ws) (ps/s)	-0.420	-1.225	-1.704	-1.35558	0.6
Relative net rate w.r.t MIT (ps/s)	–	-0.805	-1.284	-0.93558	1.02

Table 3: Correlator clock models.

Quantity	MIT	Bonn	Vienna	WACO	Shanghai
K2 Y-X delay offset (ns)	0.141 ± 0.002	0.138 ± 0.002	0.138 ± 0.002	0.137 ± 0.0	0.139 ± 0.002
Ws Y-X delay offset (ns)	-0.057 ± 0.003	-0.060 ± 0.003	-0.062 ± 0.003	-0.057 ± 0.0	-0.059 ± 0.002
K2 Y-X phase offset (deg)	-44.2 ± 3.7	-45.2 ± 2.5	-44.6 ± 3.8	-44.7 ± 1.3	-45.7 ± 3.2
Ws Y-X phase offset (deg)	-132.8 ± 4.0	-133.7 ± -2.6	-135.0 ± 4.4	-135.1 ± 3.3	-134.6 ± 3.5

Table 4: Y-X polarization delay and phase offsets set for each station by correlator.

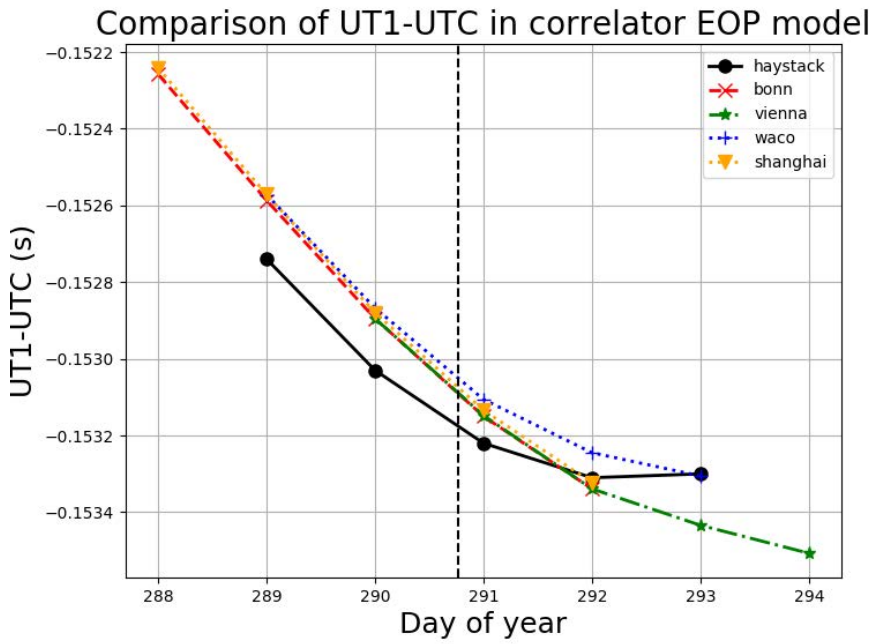

Figure 1: Value of UT1-UTC from the EOP model of each correlator. The vertical black dashed line marks the start of VI9290.

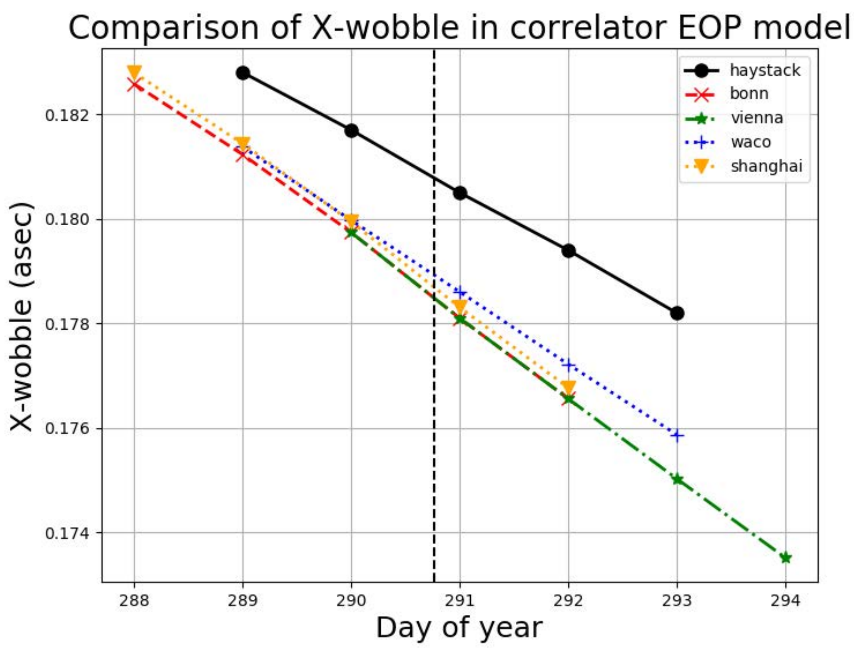

Figure 2: Value of the X-wobble parameter from the EOP model of each correlator. The vertical black dashed line marks the start of VI9290.

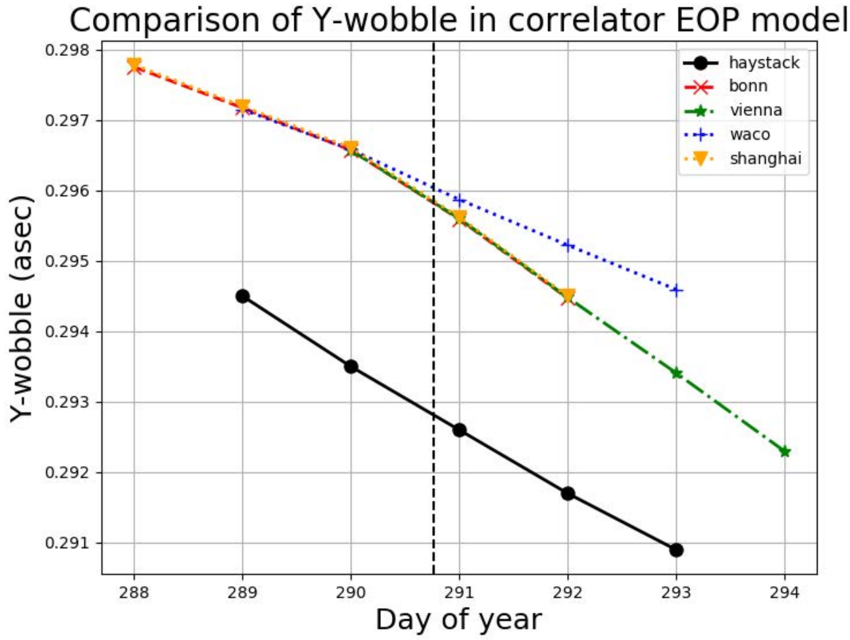

Figure 3: Value of the Y-wobble parameter from EOP model of each correlator. The vertical black dashed line marks the start of VI9290.

Correlator	Scans correlated	Number of scans with quality code:	9	8	7	≤ 6
MIT	50		25	19	5	1
Bonn	50		24	20	5	1
Vienna	50		24	19	5	2
WACO	42		20	10	9	3
Shanghai	47		24	18	4	1

Table 5: Summary of the quality codes reported for the data processing performed at each correlator.

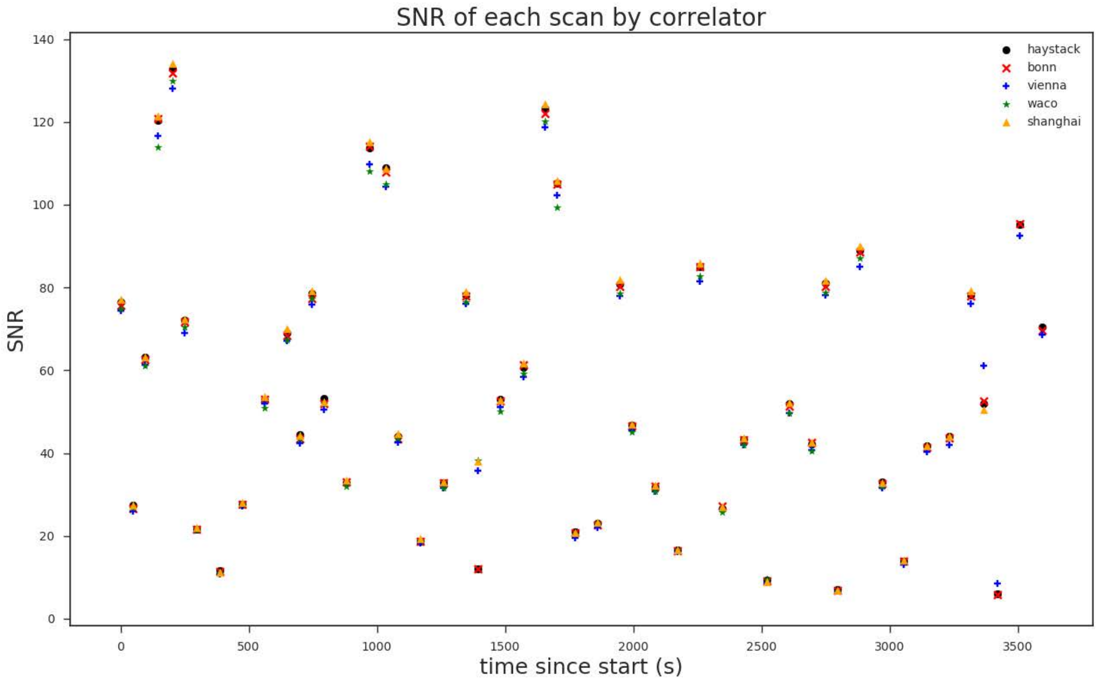

Figure 4: SNR of each scan (pseudo Stokes-I) as a function of time since the start of VI9290 for data processed by each correlator.

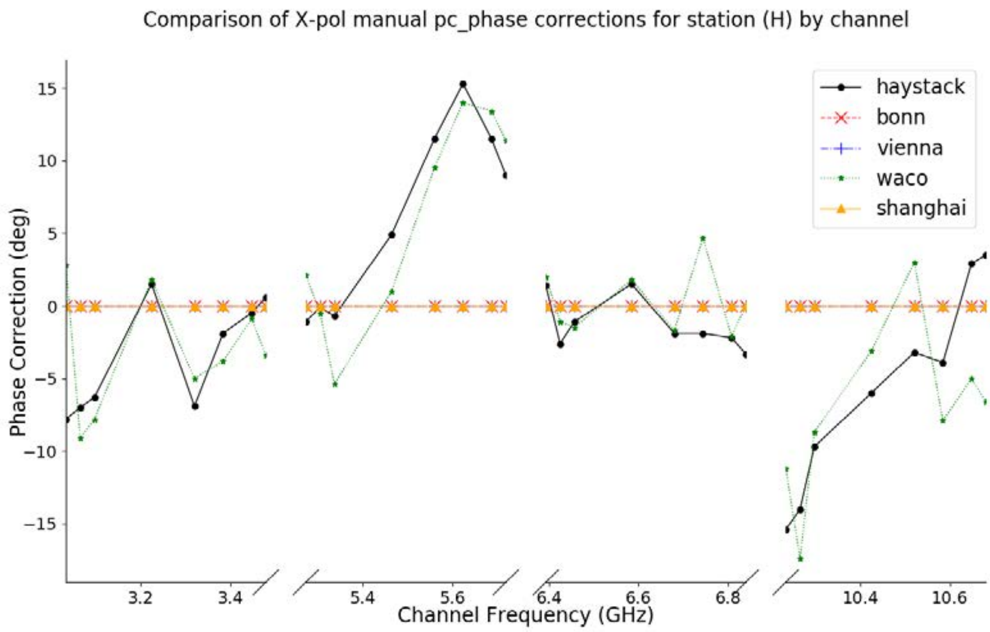

Figure 5: Manual phase-cal. (pc_phases) applied to station H (K2, Kokee) X-polarization by each correlator for all channels.

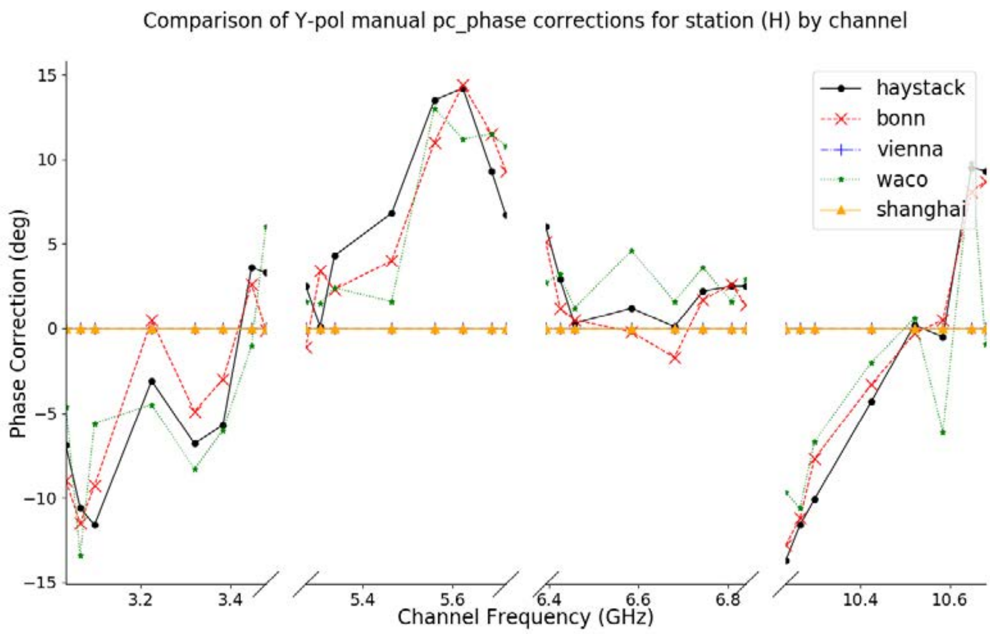

Figure 6: Manual phase-cal. (pc_phases) applied to station H (K2, Kokee) Y-polarization by each correlator for all channels.

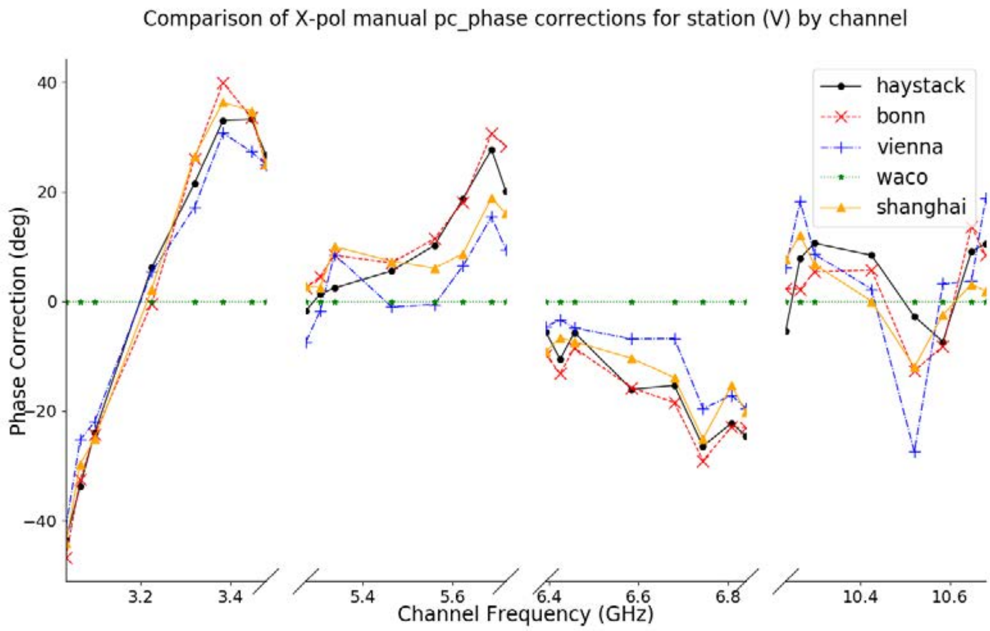

Figure 7: Manual phase-cal. (pc_phases) applied to station V (Ws, Wettzell-South) X-polarization by each correlator for all channels.

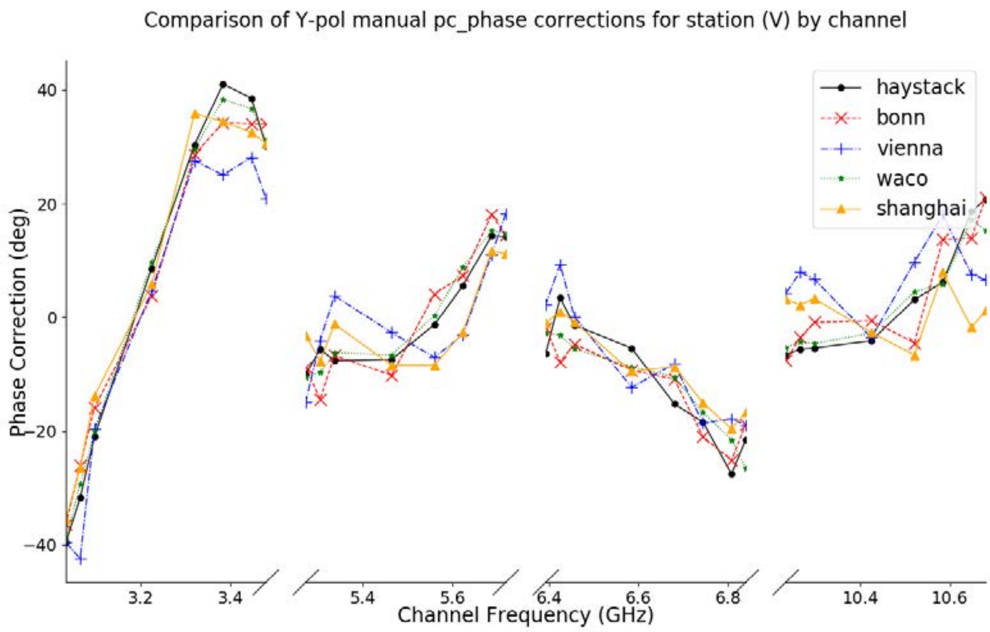

Figure 8: Manual phase-cal. (pc_phases) applied to station V (Ws, Wettzell-South) Y-polarization by each correlator for all channels.

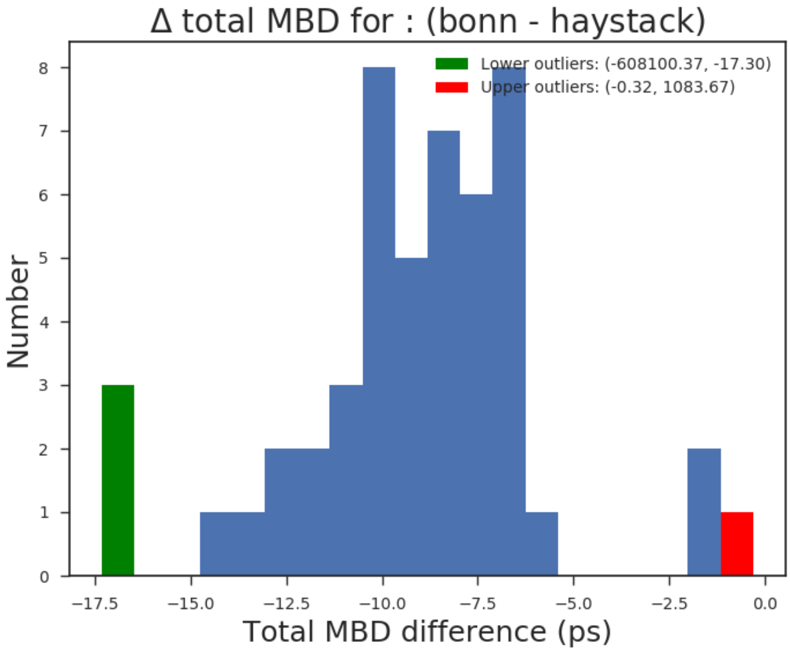

Figure 9: Histogram of the total multi-band delay difference ($\Delta\tau_{MBD}$) evaluated from each scan by MIT and Bonn. Outliers which are below (above) the lower (upper) limit of the window are shown by the green (red) bar. The height of the green (red) bar denotes the number of outliers, while the annotation denotes the range spanned by the outliers.

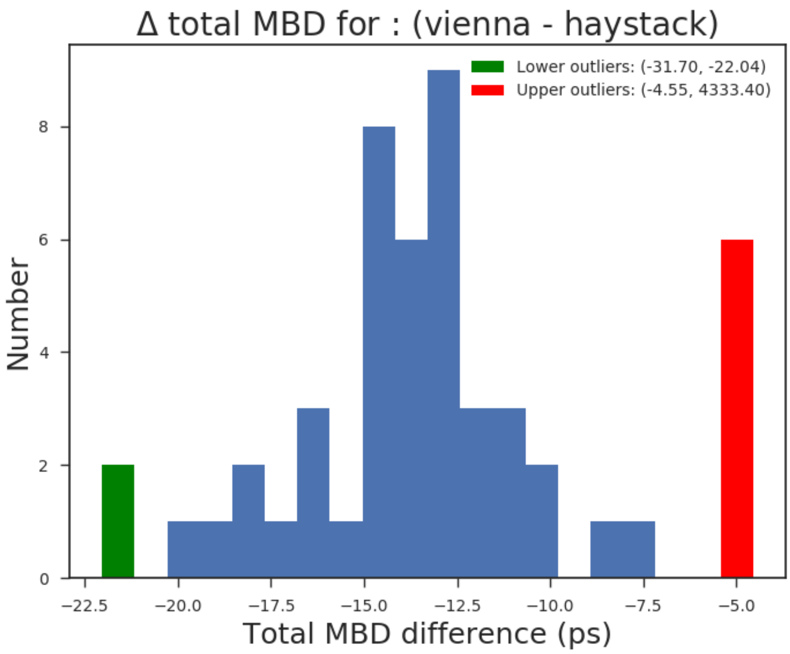

Figure 10: Histogram of the total multi-band delay difference ($\Delta\tau_{MBD}$) evaluated from each scan by MIT and Vienna. Outliers which are below (above) the lower (upper) limit of the window are shown by the green (red) bar. The height of the green (red) bar denotes the number of outliers, while the annotation denotes the range spanned by the outliers.

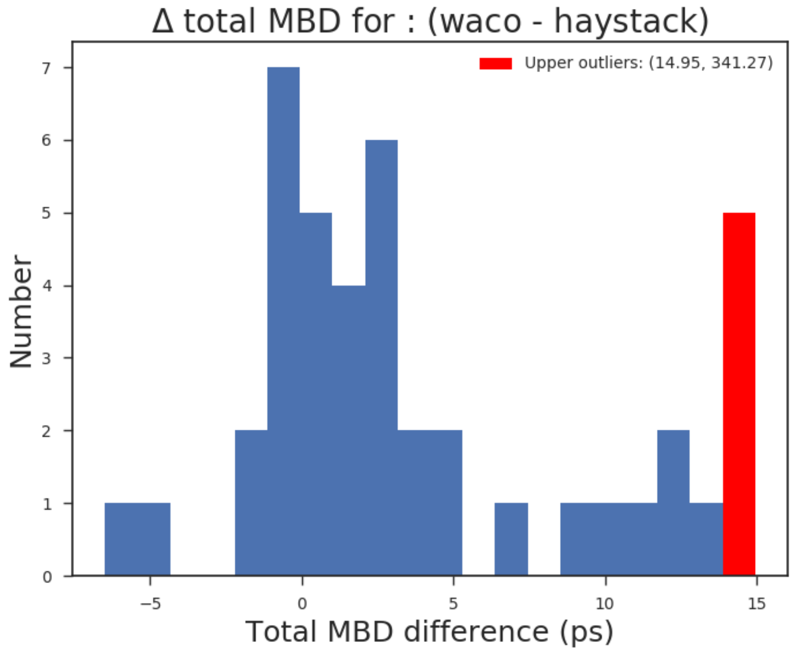

Figure 11: Histogram of the total multi-band delay difference ($\Delta\tau_{MBD}$) evaluated from each scan by MIT and WACO. Outliers which are below (above) the lower (upper) limit of the window are shown by the green (red) bar. The height of the green (red) bar denotes the number of outliers, while the annotation denotes the range spanned by the outliers.

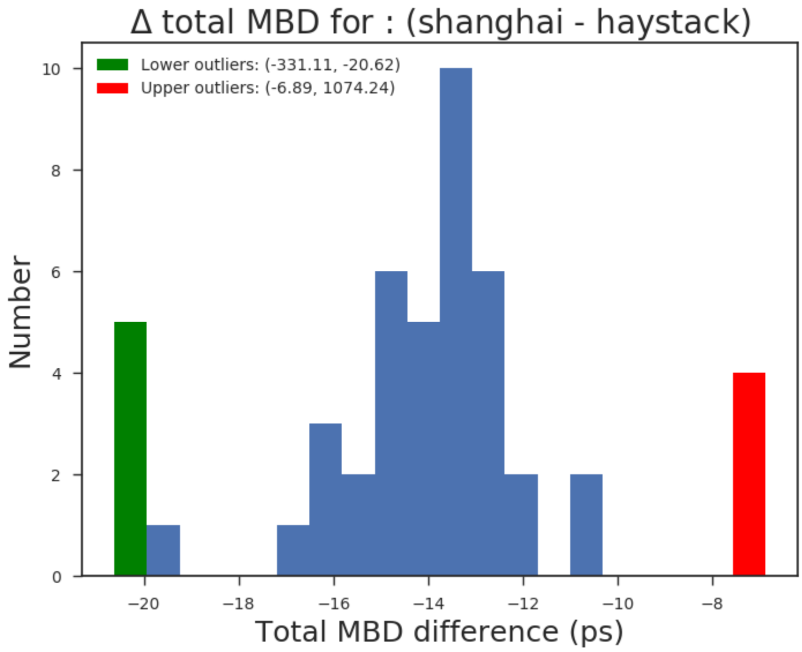

Figure 12: Histogram of the total multi-band delay difference ($\Delta\tau_{MBD}$) evaluated from each scan by MIT and Shanghai. Outliers which are below (above) the lower (upper) limit of the window are shown by the green (red) bar. The height of the green (red) bar denotes the number of outliers, while the annotation denotes the range spanned by the outliers.

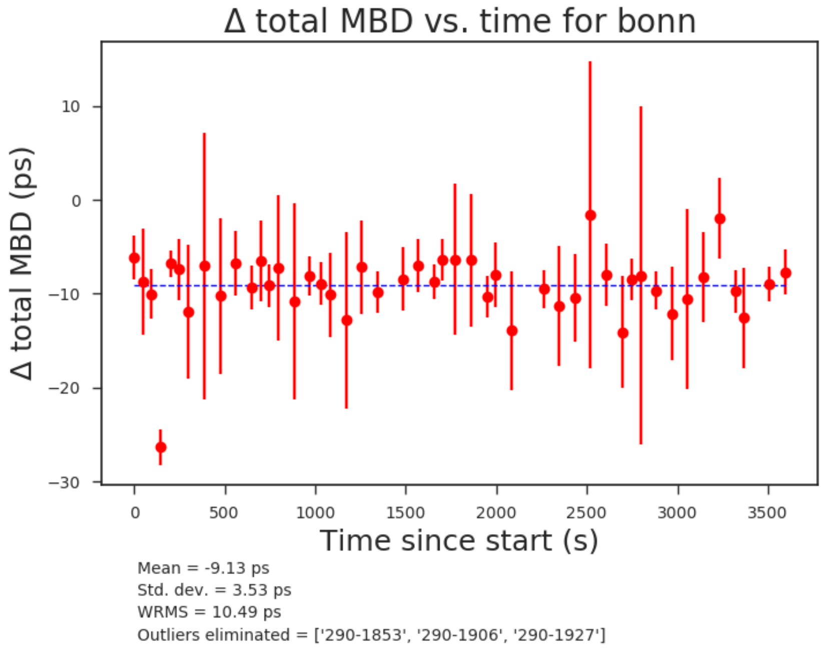

Figure 13: Plot of the total multi-band delay difference ($\Delta\tau_{MBD}$) evaluated from each scan by MIT and Bonn as a function of time since the start of the session. Outlier scans are not shown and not included in the statistics but are listed in the annotation. Mean and standard deviation are unweighted, error bars are the estimated MBD error from fourfit.

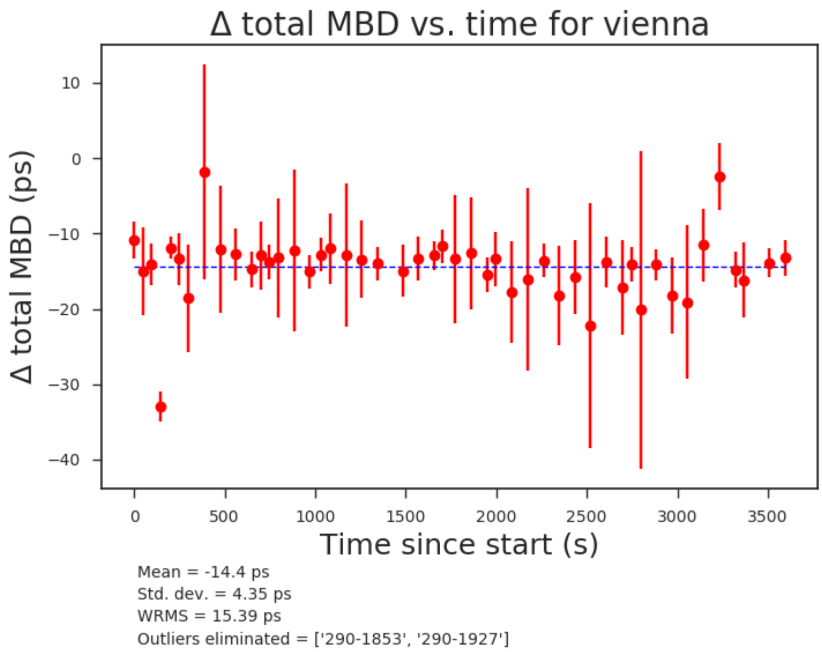

Figure 14: Plot of the total multi-band delay difference ($\Delta\tau_{MBD}$) evaluated from each scan by MIT and Vienna as a function of time since the start of the session. Outlier scans are not shown and not included in the statistics but are listed in the annotation. Mean and standard deviation are unweighted, error bars are the estimated MBD error from fourfit.

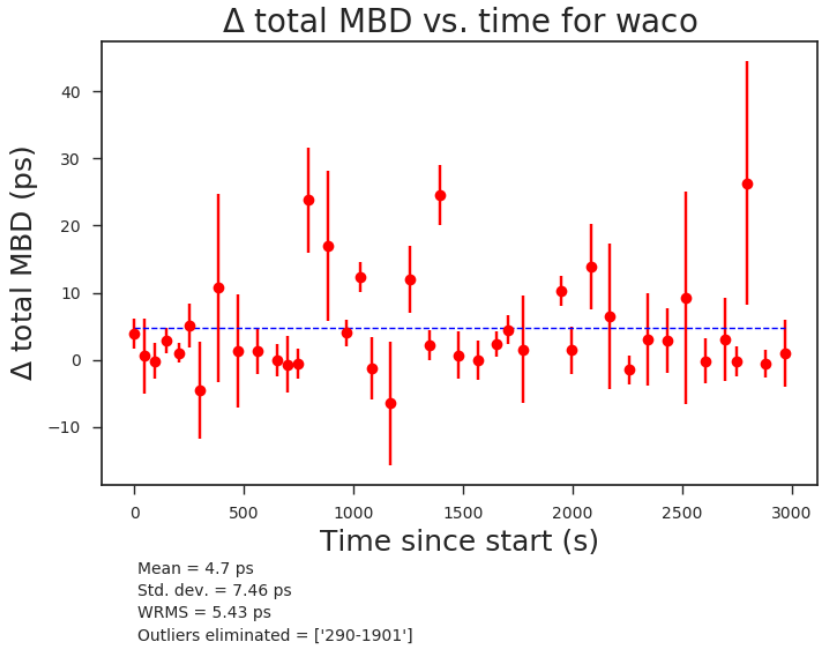

Figure 15: Plot of the total multi-band delay difference ($\Delta\tau_{MBD}$) evaluated from each scan by MIT and WACO as a function of time since the start of the session. Outlier scans are not shown and not included in the statistics but are listed in the annotation. Mean and standard deviation are unweighted, error bars are the estimated MBD error from fourfit.

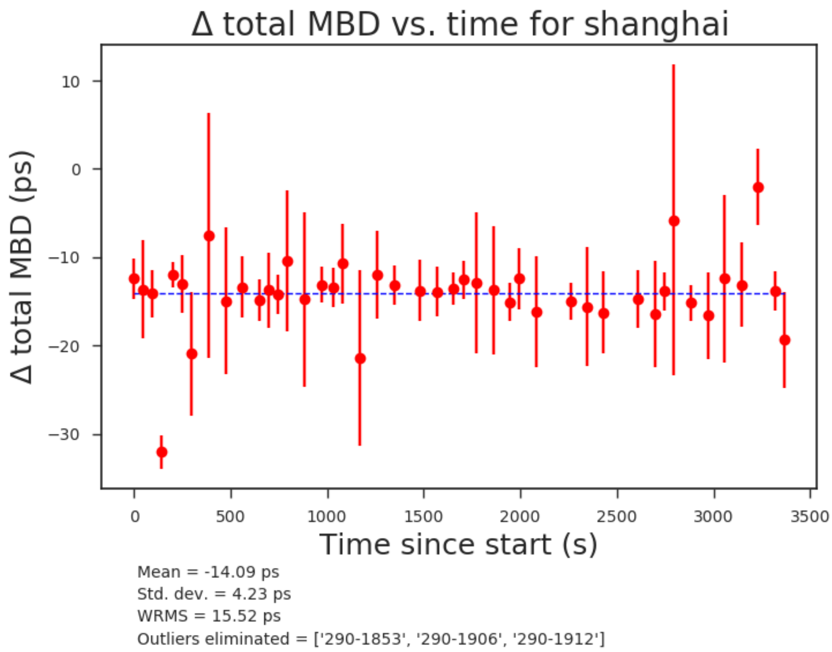

Figure 16: Plot of the total multi-band delay difference ($\Delta\tau_{MBD}$) evaluated from each scan by MIT and Shanghai as a function of time since the start of the session. Outlier scans are not shown and not included in the statistics but are listed in the annotation. Mean and standard deviation are unweighted, error bars are the estimated MBD error from fourfit.

scan	source	correlator	dTEC	quality	SNR	τ_{MBD} (μs)	$\Delta\tau_{MBD}$ (ps)
290-1853	1053+815	MIT	3.5	9	12.01	-3048.56032293	–
		Bonn	-1.59	9	11.96	-3048.56065272	-329.8
		Vienna	4.04	9	38.14	-3048.56029838	24.6
		WACO	3.75	9	35.77	-3048.56031232	10.6
		Shanghai	-1.3	9	37.95	-3048.56065404	-331.1
290-1901	0602+673	MIT	2.94	9	23.13	-216.416322403	–
		Bonn	2.74	9	22.68	-216.416328845	6.4
		Vienna	8.08	9	23.08	-216.415981136	341.3
		WACO	2.51	9	21.77	-216.416334821	-12.4
		Shanghai	2.54	9	23.28	-216.416336144	-13.74
290-1906	NGC6251	MIT	-19.46	9	16.54	-8579.58341394	–
		Bonn	9.56	9	16.32	-8579.58233027	1083.7
		Vienna	-19.34	9	16.62	-8579.58340746	6.5
		WACO	-19.75	9	16.12	-8579.58342989	-15.9
		Shanghai	9.27	9	16.53	-8579.5823397	1074.24
290-1912	1308+554	MIT	-0.91	9	9.34	6576.99013268	–
		Bonn	-0.92	9	9.04	6576.99013105	-1.63
		Vienna	-1.32	9	8.68	6576.99011041	22.27
		Waco	-0.71	9	9.55	6576.99014188	9.2
		Shanghai	-5.25	9	8.87	6576.98982308	-309.6
290-1927	1308+554	MIT	-37.44	0	5.95	7464.31676038	–
		Bonn	83.06	0	5.86	7463.70866001	-608100.0
		Vienna	-0.87	9	8.46	7464.32109378	4333.4

Table 6: Summary of scans which have been flagged as outliers based on the difference between total multi-band delay ($\Delta\tau_{MBD}$) with respect to the reference correlator (MIT Haystack). For this table, the scan data of each correlation center was fringe fit with its own respective control file. Scans/correlators where $\Delta\tau_{MBD} > 100$ps are highlighted in red. The reason for the extremely large values of $\Delta\tau_{MBD}$ for 290-1927 is likely due to corruption of the station VDIF data during a de-muxing step done before correlation. This issue may have also affected other scans, namely 290-1853 where the SNR for MIT and Bonn is much lower than Vienna/WACO/Shanghai. The other outliers appear to be associated with a disagreement in the dTEC value, though the underlying cause of this may also be due to data corruption.

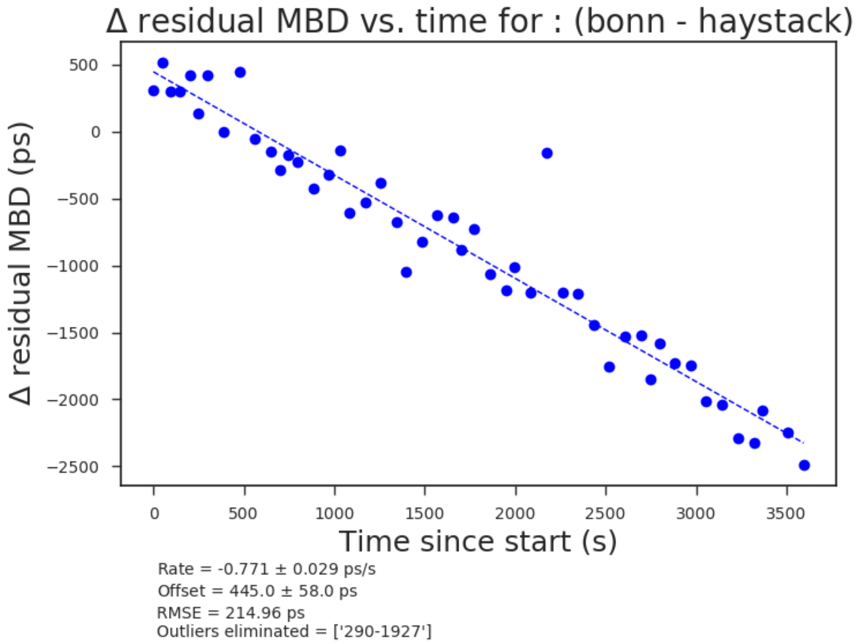

Figure 17: Plot of the residual multi-band delay difference evaluated from each scan by MIT and Bonn as a function of time since the start of the session. Outliers are not shown and not included in the linear fit. Note that the residual rate of -0.771 ± 0.029 ps/s is roughly consistent ($< 3\sigma$) with the relative net rate between the MIT and Bonn clock model of -0.805 ps/s.

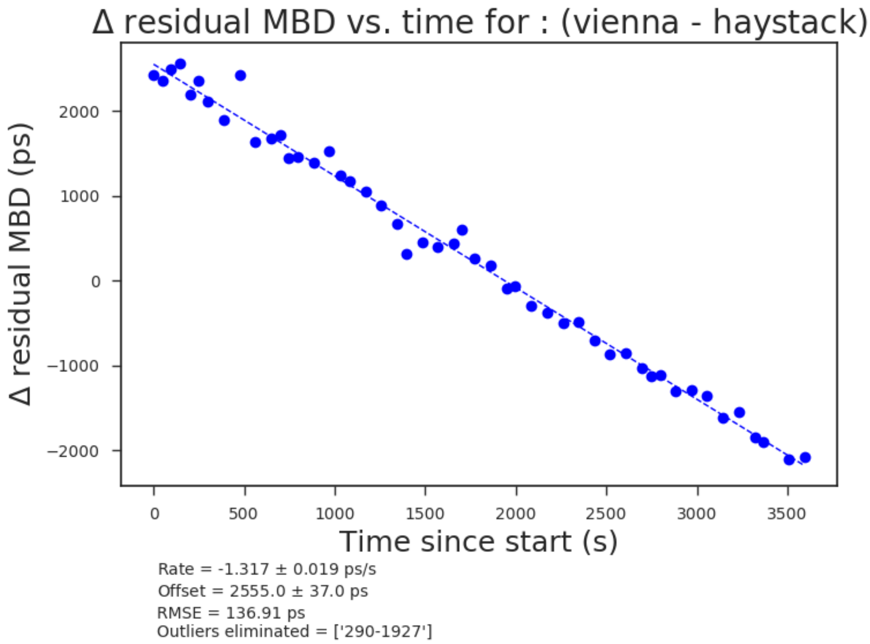

Figure 18: Plot of the residual multi-band delay difference evaluated from each scan by MIT and Vienna as a function of time since the start of the session. Outliers are not shown and not included in the linear fit. Note that the residual rate of -1.317 ± 0.019 ps/s is roughly consistent ($< 3\sigma$) with the relative net rate between the MIT and Vienna clock model of -1.284 ps/s.

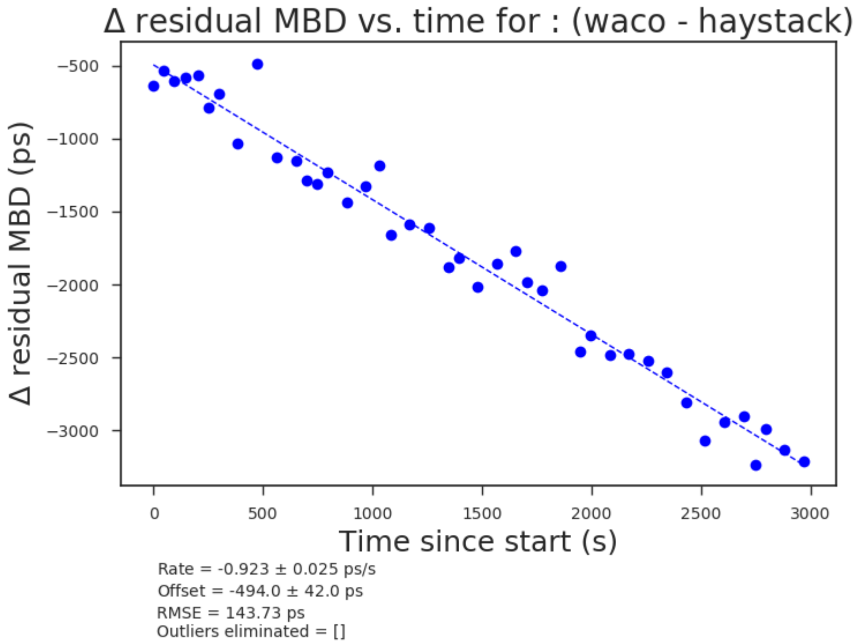

Figure 19: Plot of the residual multi-band delay difference evaluated from each scan by MIT and WACO as a function of time since the start of the session. Outliers are not shown and not included in the linear fit. Note that the residual rate of -0.923 ± 0.025 ps/s is roughly consistent ($< 3\sigma$) with the relative net rate between the MIT and WACO clock model of -0.936 ps/s.

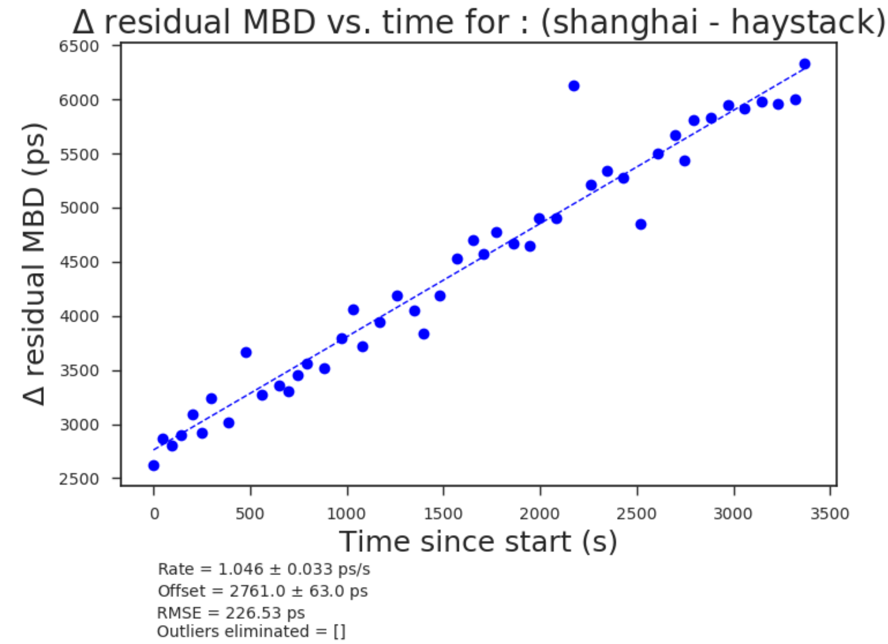

Figure 20: Plot of the residual multi-band delay difference evaluated from each scan by MIT and Shanghai as a function of time since the start of the session. Outliers are not shown and not included in the linear fit. Note that the residual rate of 1.046 ± 0.033 ps/s is roughly consistent ($< 3\sigma$) with the relative net rate between the MIT and Shanghai clock model of 1.02 ps/s.

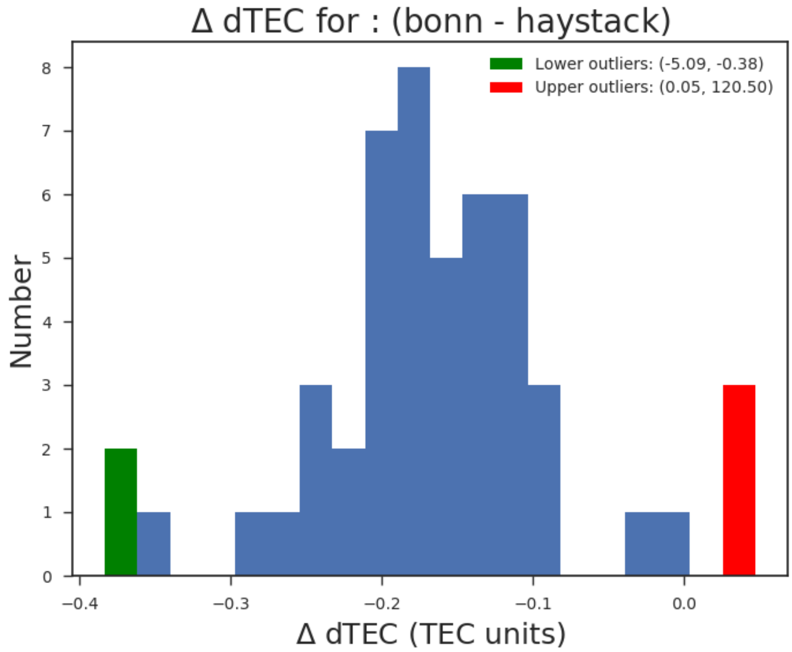

Figure 21: Histogram of the differences between the dTEC evaluated from each scan by MIT and Bonn. Outliers which are below (above) the lower (upper) limit of the window are shown by the green (red) bar. The height of the green (red) bar denotes the number of outliers, while the annotation denotes the range spanned by the outliers.

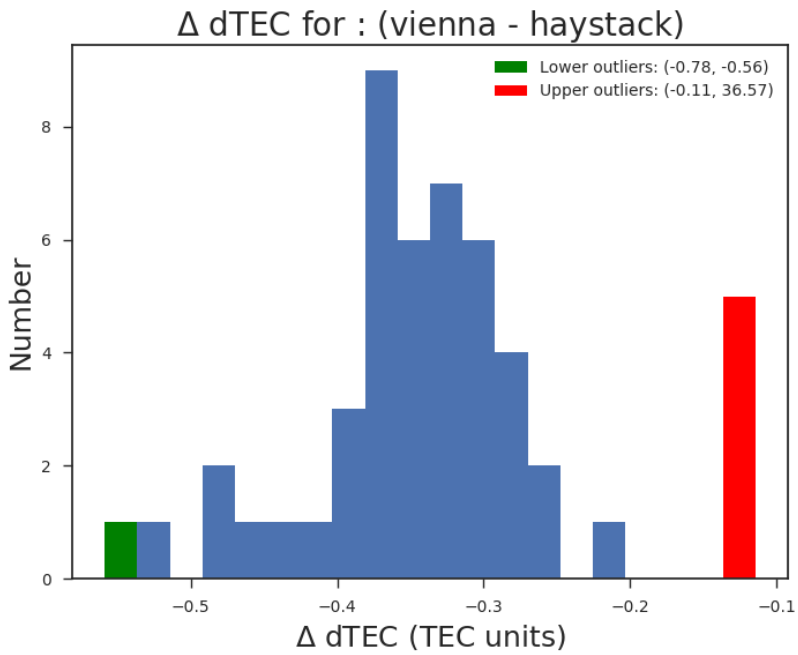

Figure 22: Histogram of the differences between the dTEC evaluated from each scan by MIT and Vienna. Outliers which are below (above) the lower (upper) limit of the window are shown by the green (red) bar. The height of the green (red) bar denotes the number of outliers, while the annotation denotes the range spanned by the outliers.

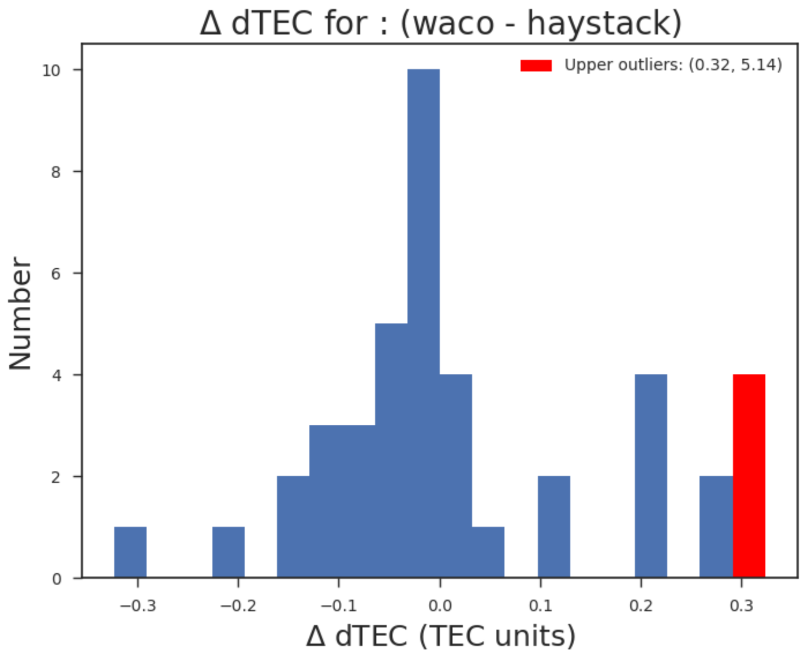

Figure 23: Histogram of the differences between the dTEC evaluated from each scan by MIT and WACO. Outliers which are below (above) the lower (upper) limit of the window are shown by the green (red) bar. The height of the green (red) bar denotes the number of outliers, while the annotation denotes the range spanned by the outliers.

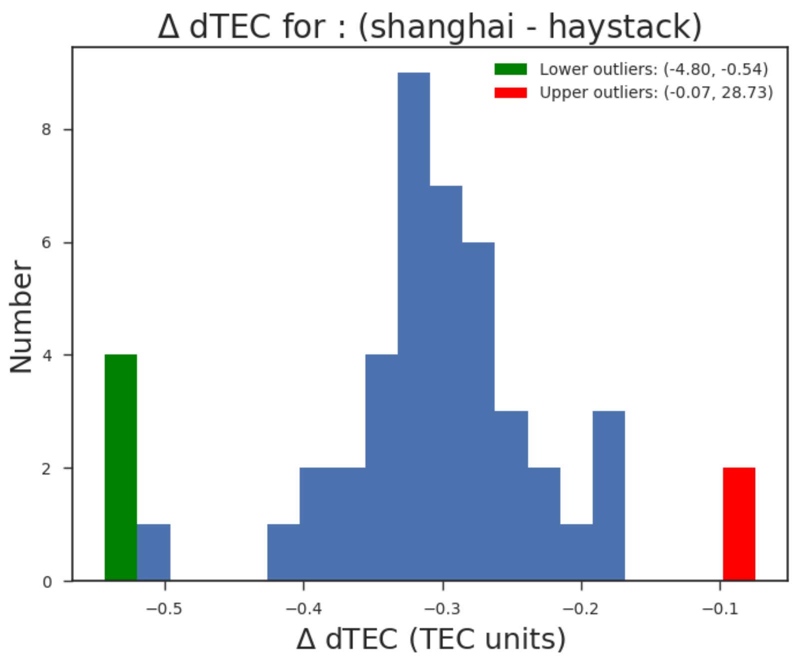

Figure 24: Histogram of the differences between the dTEC evaluated from each scan by MIT and Shanghai. Outliers which are below (above) the lower (upper) limit of the window are shown by the green (red) bar. The height of the green (red) bar denotes the number of outliers, while the annotation denotes the range spanned by the outliers.

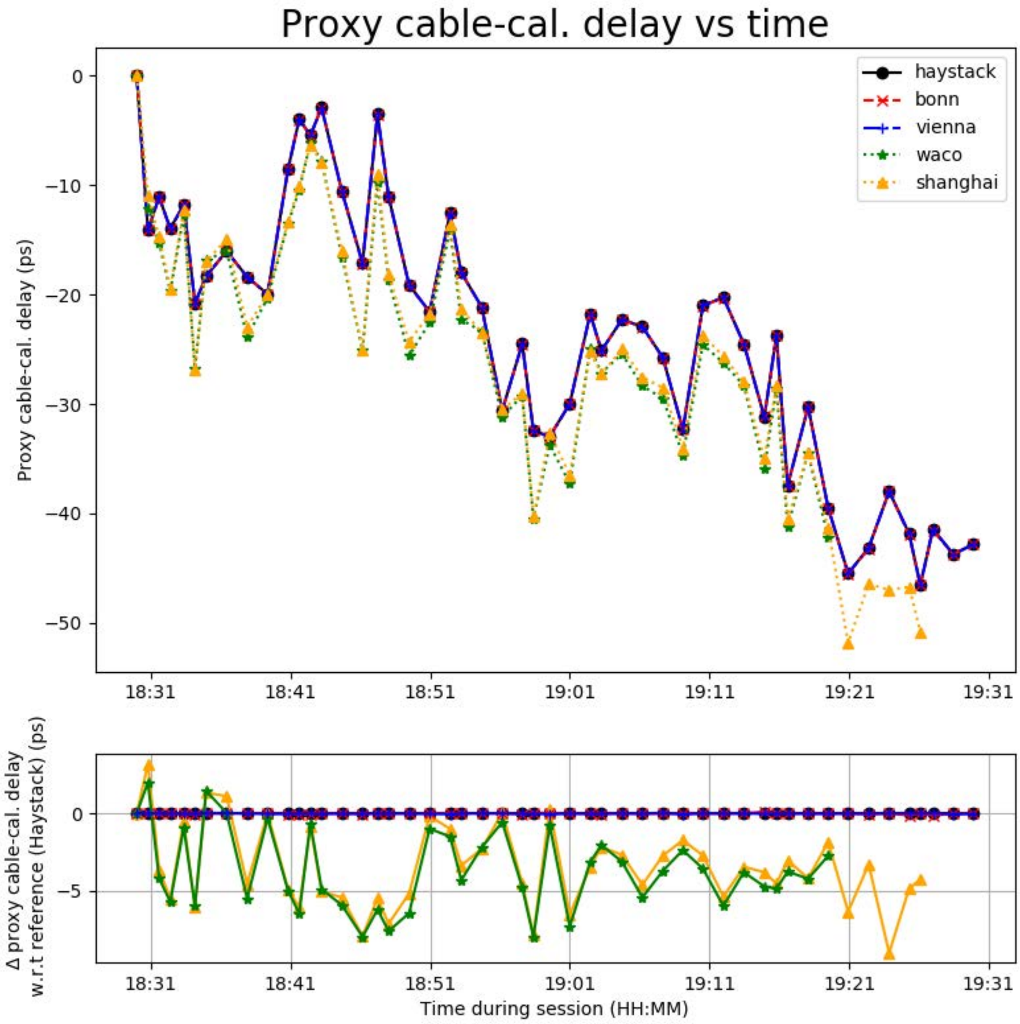

Figure 25: The proxy cable-cal delay computed by each correlator for Kokee (K2) as a function of time during VI9290.

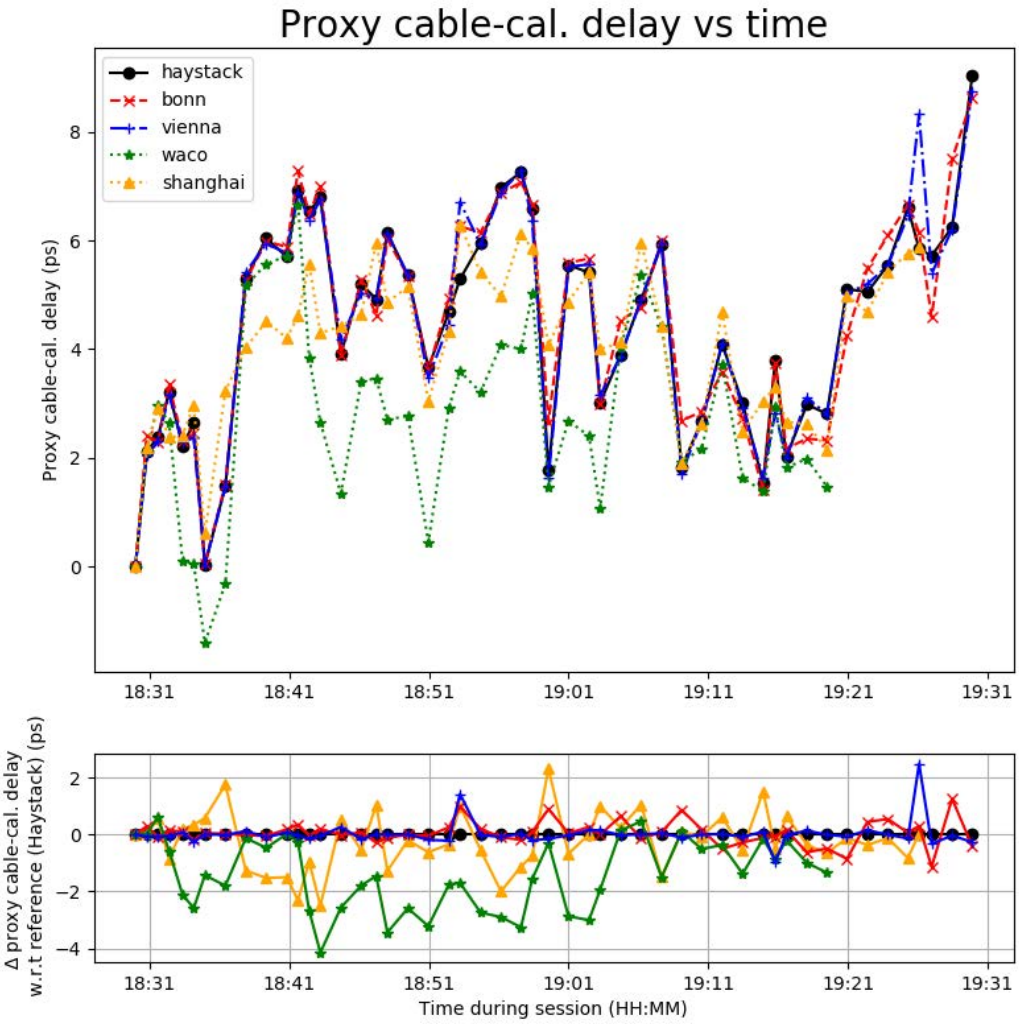

Figure 26: The proxy cable-cal delay computed by each correlator for Wettzell (Ws) as a function of time during VI9290.

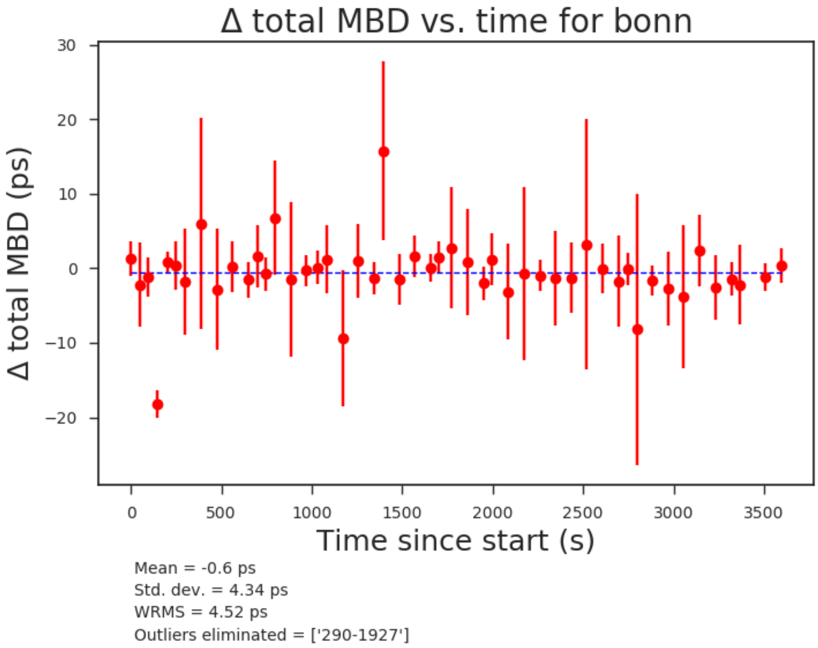

Figure 27: Plot of the total multi-band delay difference ($\Delta\tau_{MBD}$) evaluated from each scan by MIT and Bonn as a function of time since the start of the session. However, in this plot, Bonn's correlated data has been fringe-fit with MIT's control file. Outlier scans are not shown and not included in the statistics but are listed in the annotation. Mean and standard deviation are unweighted, error bars are the estimated MBD error from fourfit.

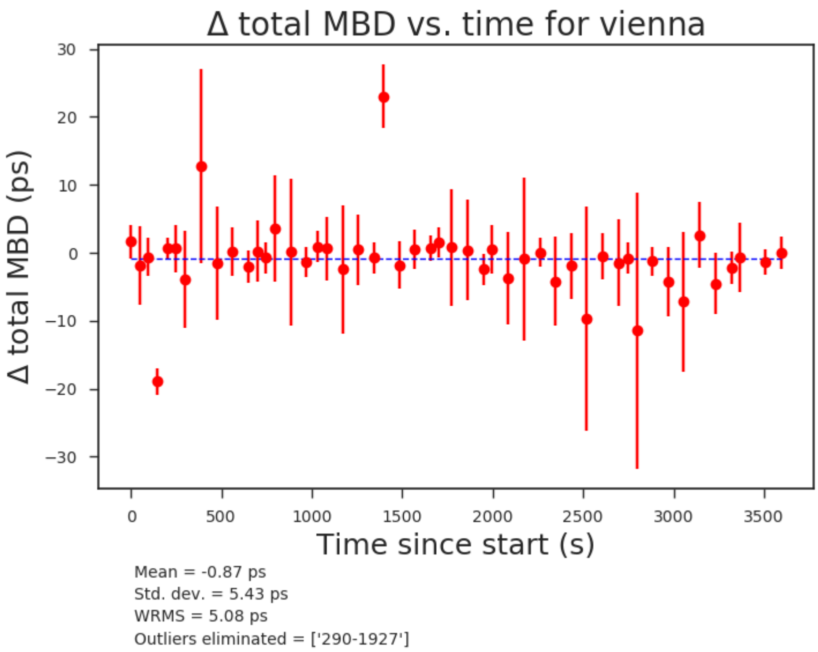

Figure 28: Plot of the total multi-band delay difference ($\Delta\tau_{MBD}$) evaluated from each scan by MIT and Vienna as a function of time since the start of the session. However, in this plot, Vienna's correlated data has been fringe-fit with MIT's control file. Outlier scans are not shown and not included in the statistics but are listed in the annotation. Mean and standard deviation are unweighted, error bars are the estimated MBD error from fourfit.

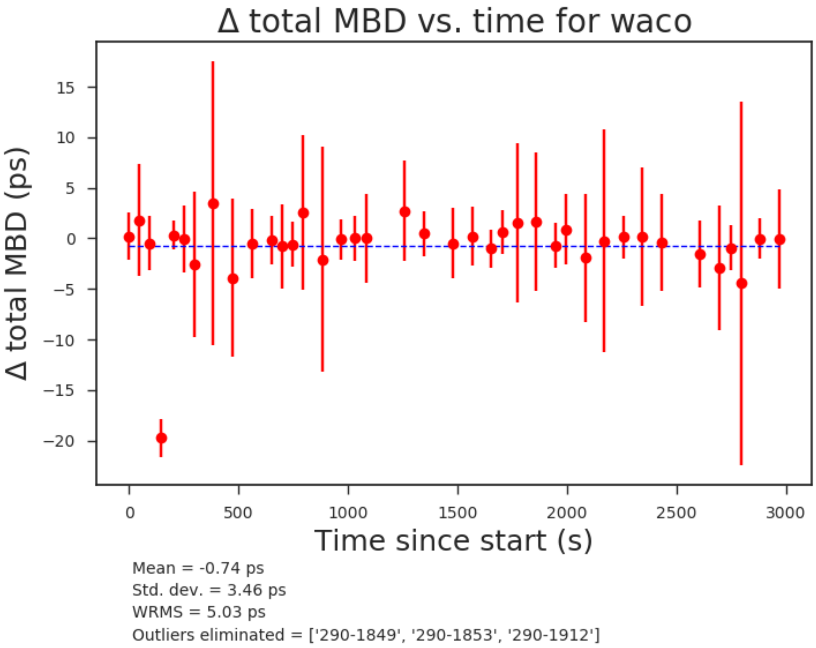

Figure 29: Plot of the total multi-band delay difference ($\Delta\tau_{MBD}$) evaluated from each scan by MIT and WACO as a function of time since the start of the session. However, in this plot, WACO's correlated data has been fringe-fit with MIT's control file. Outlier scans are not shown and not included in the statistics but are listed in the annotation. Mean and standard deviation are unweighted, error bars are the estimated MBD error from fourfit.

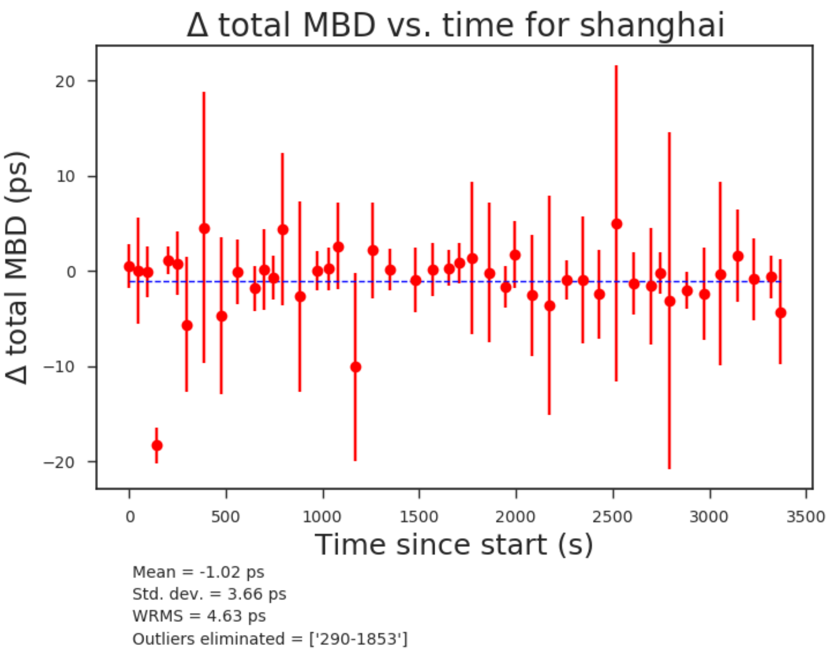

Figure 30: Plot of the total multi-band delay difference ($\Delta\tau_{MBD}$) evaluated from each scan by MIT and Shanghai as a function of time since the start of the session. However, in this plot, Shanghai's correlated data has been fringe-fit with MIT's control file. Outlier scans are not shown and not included in the statistics but are listed in the annotation. Mean and standard deviation are unweighted, error bars are the estimated MBD error from fourfit.

Correlator	Control file	Mean offset (ps)	Std. dev. (ps)	WRMS (ps)
Bonn	Bonn's	-9.13	3.53	10.49
Vienna	Vienna's	-14.4	4.35	15.39
WACO	WACO's	4.7	7.46	5.43
Shanghai	Shanghai's	-14.09	4.23	15.52
Bonn	MIT's	-0.6	4.34	4.52
Vienna	MIT's	-0.87	5.43	5.08
WACO	MIT's	-0.74	3.46	5.03
Shanghai	MIT's	-1.02	3.66	4.63

Table 7: Summary of parameters describing the total multi-band delay differences between each correlators' data and the reference correlator, where the data has been fringe fit using the listed control file. The reference value for τ_{MBD} is determined from MIT's data fringe fit with MIT's control file.